# INFLUENCE OF THE DISTRIBUTION OF NON-CONDENSIBLES ON PASSIVE CONTAINMENT CONDENSER PERFORMANCE IN PANDA

*Th. Bandurski, M. Huggenberger, J. Dreier, C. Aubert, F. Putz,*
*R.E. Gamble, G. Yadigaroglu*

*Recently, passive cooling systems have been designed for the long-term decay heat removal from the containment of Advanced Light Water Reactors. In particular, the long-term LOCA response of the Passive Containment Cooling System (PCCS) for the General Electric European Simplified Boiling Water Reactor (ESBWR) has been tested in the large-scale PANDA facility. The PANDA tests achieved the dual objectives of improving confidence in the performance of the passive heat removal mechanisms underlying the design of the system, and extending the data base available for containment analysis code qualification. The tests conducted subject the PCCS to a variety of conditions representing design-basis and beyond-design-basis accident conditions. These include operation in the presence of both heavier and lighter than steam non-condensible gases, as well as a variety of asymmetric and challenging start-up conditions. The present paper addresses the transient distribution of non-condensibles in PANDA, and their effect on (passive) condenser performance.*

## 1 INTRODUCTION

Within the framework of the Euratom Fourth Framework Project "Technology Enhancement for Passive Safety Systems" (TEPSS), a PANDA test programme has been conducted at the Paul Scherrer Institut in Switzerland. The goal of this programme was the experimental investigation of the long-term decay heat removal from the containment of the European Simplified Boiling Water Reactor (ESBWR).

Passive safety systems have become an element in certain Advanced Light Water Reactor (ALWR) designs, in particular with regard to containment cooling. The aim in introducing passive systems in nuclear power plants (NPPs) is to increase the reliability of the safety systems, to simplify the design of the plant and, eventually, to reduce investments and operational costs.

Passive systems function on the basis of physical phenomena like natural circulation, fluid mixing and stratification, heat conduction etc. On the one hand, the design of passive systems has to meet certain requirements for the expected physical phenomena to take place. To prove that these requirements are met, the design needs experimental confirmation. On the other hand, passive systems, unlike active systems, cannot be easily launched, but will only be initiated when the underlying driving mechanisms are established, e.g. temperature, density and/or pressure differences. As a consequence, the effectiveness of some passive safety systems cannot be easily demonstrated in real NPPs.

For these reasons, system tests are required for the certification of passive safety systems. The tests can be performed in facilities which have to be correctly scaled to make sure that the phenomena underlying the design concept will be properly observed in these tests. Experiments carried out in test facilities give evidence of the performance in scaled systems. The data obtained from scaled tests is also used for model and code assessment which, again, assumes a comprehensive and detailed understanding of the observations so that all significant phenomena can be taken into consideration with confidence. Finally, welll assessed codes can be applied to system behavior analyses for real nuclear installations.

The purpose of passive containment cooling systems is to remove the energy released from the system components under accident conditions to the environment while guaranteeing containment integrity. The key parameters characterizing the integrity of an ALWR containment, particularly during the long-term decay heat removal phase, are peak system pressures and temperatures. Beyond this, assuming severe accident conditions, the distribution of hydrogen is of interest because of its explosive character in mixtures with oxygen; the ESBWR containment considered here is, however, inerted with a nitrogen atmosphere.

The containment pressure is mainly determined from the performance of the containment cooling system, and by the amount and transient distribution of non-condensible gases filling initially the containment compartments (nitrogen or air) or being released later in the course of the transient from the reactor core (hydrogen). The containment temperatures are mainly influenced by the steam and non-condensible gas distribution in the containment compartments, i.e by gas mixing and stratification phenomena in large volumes. The distribution of steam, air and their mixtures in and between containment compartments was, for example, observed in several large-scale PANDA system tests. However, only recently has the first system behaviour test with helium been performed in PANDA.

The ESBWR designed by General Electric (GE) employs vertical-tube condensers immersed in pools on top of the containment to limit the system pressure increase by condensing steam out of the gas mixture fed to the condensers from the containment atmosphere. The Passive Containment Condensers (PCCs) resemble the Isolation Condensers (ICs) used in certain boiling water reactor plants for decay heat removal during isolation events. One of the main differences between the two systems is the large

amount of non-condensible gases which can be conveyed to the condenser surface of the PCCs.

The condenser efficiency depends critically on the non-condensible gas concentration at the condenser surface. To prevent the blockage of the condenser tubes with non-condensible gases, vent lines are connected to the PCC lower headers. The other ends of the vent lines are submerged in the Suppression Pool (SP). Insufficient energy removal in the PCCs leads to Drywell pressure increase and, eventually, the non-condensible gases are vented to the space above the SP (Shiralkar, 1997).

With regard to system behavior, the PCC venting mechanism is well understood from former PANDA tests for mixtures of saturated steam and non-condensible gases heavier than steam, e.g. air. The mixture, supplied to the PCC upper header, passes downwards through the vertical condenser tubes. While steam is condensing, the air fraction and density of the mixture are increasing. From the lower header, the mixture with the highest air fraction, highest density and lowest temperature, is vented. Furthermore, the condensers adjust their performance with decreasing decay power by accumulating non-condensibles heavier than steam in the lower part of the condenser tubes and thereby reducing the effective condensing length.

However, assuming severe accident conditions, non-condensible gases lighter than steam, i.e. hydrogen, have to be considered. In PANDA tests, hydrogen was replaced by helium. Unlike in steam/air mixtures, in the parameter range of interest the density of gas mixtures consisting of saturated steam and helium decreases with increasing helium content. Therefore, the buoyancy forces arising from steam condensation from a steam/helium mixture in the vertical PCC tubes do not support the desired gas movement from the upper to lower header, and on through the PCC vent lines to the suppression chamber (SC). The influence of helium on condenser performance was investigated in the full-scale PCC test facility PANTHERS. However, in complementary tests, the PANDA PCC performance has also been investigated in a first-of-a-kind, large-scale system behaviour test with helium injection.

The present paper focuses on two major aspects of the experimental evaluation of the ESBWR PCC performance in the PANDA facility. These are gas mixing and stratification in large volumes, and PCC performance in the presence of non-condensible gases lighter than steam (helium). A brief interpretation of the measured data, in particular with regard to PCC performance, will also be given. The observations obtained in the PANDA test in which helium was injected late in the transient are compared with results from a test simulating hidden air release in the DW, also late in the transient.

## 2 PANDA FACILITY AND TEST SCENARIOS

PANDA is a large-scale, multipurpose test facility, and has been used to investigate, in particular, long-term, passive containment cooling systems for different designs. With regard to modern ALWR containment designs, PANDA scales heights approximately 1:1 and, in particular, decay power and volumes 1:40 for the ESBWR. The facility consists of large interconnected vessels and open pools, and provides appropriate conditions for buoyancy-driven and multi-dimensional phenomena to be investigated. Prototypical fluids, such as water and steam, as well as close-to-prototypical fluids, are used. Non-condensible gases heavier (air) and lighter (helium) than steam were used in the tests. Detailed information on PANDA scaling with regard to the SBWR and ESBWR can be found in Yadigaroglu (1996) and Schenk (1997). The facility is well instrumented with regard to system behaviour evaluation. The instrumentation comprises instruments for fluid and wall temperature measurements, total and partial air pressures, pressure differences, flow meters, phase indicators, valve states, and heater power. More information on earlier test programmes and instrumentation can be found in Bandurski (1997) and Yadigaroglu (1998).

Briefly, the configuration of the PANDA facility for investigating the ESBWR PCCs can be described as follows. There are six vertical, cylindrical vessels, four water pools, and a variety of connecting lines available to compose different facility configurations. Two pairs of interconnected vessels and four water pools are arranged to form the SC, DW and cooling water storage for the condensers. The SC vessels are connected in the gas-filled region, and in the water region. Another tank is used to represent the reactor pressure vessel (RPV), and another the Gravity Driven Cooling System (GDCS) storage tank. In the ESBWR configuration, the GDCS and SC gas spaces are connected. The RPV serves as a steam source: i.e., the RPV water is heated by controlled electrical heaters simulating the core. PCC vent lines and main vent lines (MVL), submerged in the SP, are connected to the condenser lower headers and DW vessels, respectively. Vacuum breakers (VBs) connect the SC and DW gas spaces. Components which were not part of a test, such as one of the PCC units in some cases, are valved off.

In PANDA, a postulated ESBWR main-steam-line break (MSLB) is simulated, since this then provides an envelope case for breaks of smaller sizes Shiralkar (1998). Briefly, the accident scenario of an ESBWR MSLB can be described as follows (Shiralkar, 1998). During the initial depressurization phase, much of the decay heat, and the energy stored in the reactor coolant and structures, is deposited in the SP. At the same time, practically all non-condensibles contained in the DW are conveyed to the SC gas space. Following initial depressurization, the GDCS water can be discharged into the RPV.

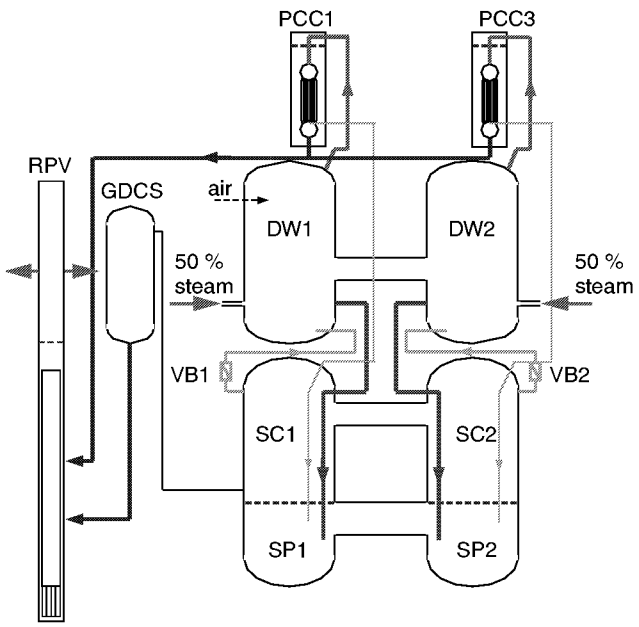


**Fig. 1:** PANDA facility configuration for Test P5

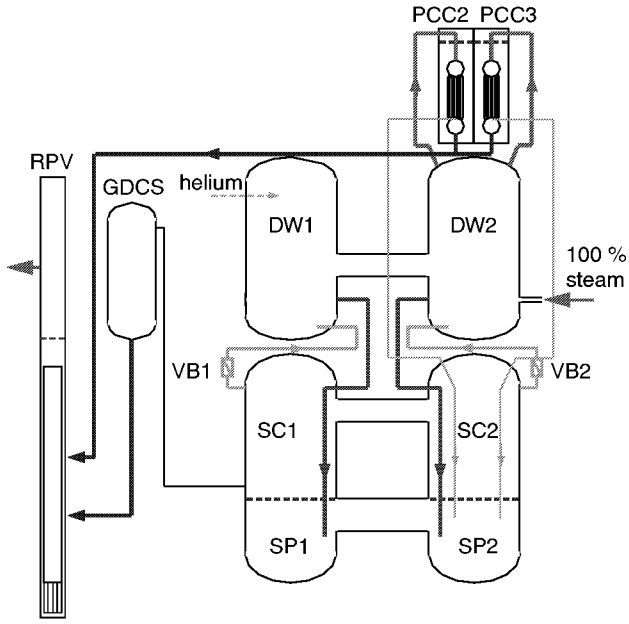


**Fig. 2:** PANDA facility configuration for Test P7

During the GDCS phase, steam generation in the RPV is interrupted, and condensation in the RPV, in the DW (due to spill-over), and in the PCCS condensers, causes the DW pressure to drop below the SC pressure. To preserve containment structural integrity, Vacuum Breakers (VBs) open to equalize the DW and SC pressures. By this means, a small amount of non-condensible gas is transported from the SC to the DW. The cold water discharged from the GDCS to the RPV is heated and, eventually, boiling resumes. At this time, the long-term containment cooling phase begins. From now on the decay heat must be removed by the PCC condensers. Resumption of boiling in the RPV was the starting time for most of the ESBWR PCC tests in PANDA.

The ESBWR PANDA tests address the long-term decay heat removal phase. A variety of conditions representing design-basis and beyond-design-basis accident conditions were simulated to challenge the PCC system. The test conditions include operation in the presence of both heavier and lighter than steam non-condensible gases, as well as asymmetric and start-up conditions. Detailed information on the test matrix, initial conditions, etc. has been published by Huggenberger (1999). Two tests are discussed in the present paper. These are Test P5, characterized by "hidden" air release into the DW late in the transient, and Test P7, simulating hydrogen (helium) release to the DW under beyond-design-accident conditions.

The PANDA facility configurations for Tests P5 and P7 are presented on Figs. 1 and 2. In Test P5, the steam generated in the RPV was symmetrically discharged into both DW vessels. One PCC unit was connected into each DW vessel. Later in the transient, air was released near the top of DW1. In Test P7, all steam was discharged to DW2, to which both operating PCC units were connected.

Later in the transient, helium was injected near the top of DW1. Test P7 was intended to investigate the system behavior and PCC performance in the presence of a gas lighter than steam rather than simulating a particular beyond-design-accident scenario. In both tests, only two PCC units were operating: i.e., the design heat removal capability of the PCCs was exceeded, at least at the beginning of the tests. The way of connecting the two PCCs, one to each DW vessel in Test P5, and both PCCs to one DW vessel in Test P7, as well as the symmetric/ asymmetric steam injection, introduces different boundary conditions in the tests. However, with regard to the main phenomena observed, Test P5 seems to be suitable for comparison with Test P7.

## 3 MIXING AND STRATIFICATION

### 3.1 Impact of Gas Mixing and Stratification on System Pressure

The overall containment system pressure is primarily determined by the performance of the PCCs and the amount of non-condensible gases which initially filled the containment compartments, or was released later during the course of the transient. The effect of PCC performance on system pressure will be discussed in Section 4. In the description of the accident scenario, it was mentioned that the non-condensibles initially filling the DW are essentially purged to the SC during the reactor depressurization phase. In the SC, the non-condensible gases are effectively trapped, and thereby determine the overall system pressure level. Only a small fraction of the non-condensibles can be returned from the SC to the DW during VB openings. Ultimately, the non-condensibles returned to the DW are mixed with the injected steam, and then conveyed to the PCCs, from where they are soon vented again, except for the very small amount needed for "adjust-

ing" the active condenser surface. Therefore, during the long-term containment cooling phase, the DWs contain essentially steam and, possibly, a very small fraction of non-condensibles.

It should be noted here that, during the long-term cooling phase, the DW to SC pressure difference can vary over a small range only. On the lower side, the pressure difference is limited by the VB settings, and its highest value is determined principally by the PCC feed line pressure drops, and by the PCC vent line submergence depth. Venting of non-condensibles from the DW to the SC causes a shift of both pressures to higher values due to the SC pressure increase. Venting of steam, which is always present in the gas mixture, can lead to temperature stratification in the SP, and consequently to an increase in the steam partial pressure in the SC gas space due to evaporation from the SP surface. However, the observations from the PANDA tests show that this effect is less significant in the long-term cooling phase.

Potentially, non-condensible gases can be released to the DW later in the transient: e.g., as hydrogen is released under severe accident conditions, or by hidden air release from DW compartments. If these non-condensible gases are mixed with the steam produced in the RPV, and/or conveyed to the PCCs, they will also be vented to the SC, and thence contribute to the system pressure increase. In this case, the SC pressure increase is essentially determined by the amount of non-condensibles added to the SC gas space. If the newly released non-condensibles accumulate in DW regions, due to gas stratification, and cannot then be transported to the PCCs, the DW pressure would only increase moderately during the injection period. However, the DW to SC pressure difference is limited, and venting could still occur. The adjustment of the active condenser heat transfer surface (which will be described in Section 4.2) would partially compensate for the DW pressure increase. If the non-condensibles can ultimately be retained in stable stratification layers, then venting stops too. Concluding, we can say that the system pressure is sensitive to mixing and stratification phenomena if non-condensible gases are released to the DW at late times in the long-term containment cooling phase. However, the system pressure increases significantly only when the non-condensibles are actually vented to the SC.

### 3.2 Observation of Gas Mixing and Stratification in Tests P5 and P7

The phenomena described qualitatively above have actually been observed in PANDA Tests P5 and P7 (see Figs. 3 and 4). In Test P7, helium was injected (4 g/s) into the upper part of DW1, four hours after test initiation, over a period of two hours. The helium mixed with steam in the upper part of DW1. The steam/helium mixture region slowly extended downwards until the upper edge of the pipe connecting the two DW vessels was reached.

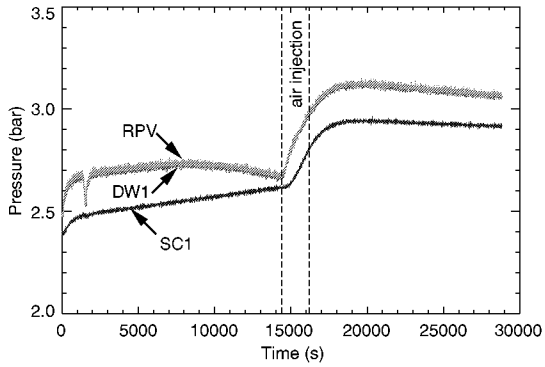


**Fig. 3:** Test P5 – pressure in DW1, SC1 and RPV

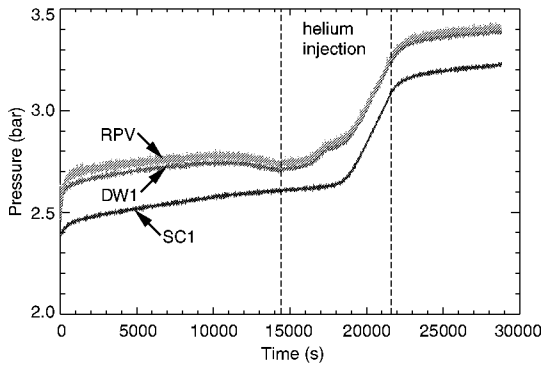


**Fig. 4:** Test P7 – pressure in DW1, SC1 and RPV

The PCC temperatures reflect the presence of helium even before the gas temperature measurement in the upper region of the DW connecting pipe, indicated that there was an overflow of relatively cold steam/helium mixture from the upper part of DW1 to DW2. In DW2, the gas was well mixed by the injected steam. Beginning with the overflow of the helium/steam mixture from DW1 to DW2, all thermocouples installed in the PCC units indicated the presence of non-condensibles. Later, helium was vented to the SC.

A slight DW pressure increase was observed from the very beginning of the helium injection phase, as shown in Fig. 4. It should be noted here that the SC pressure was essentially unaffected by the helium injection at this time. (The reason for the slight SC pressure increase is discussed in Section 3.3). The reason for the *moderate* DW pressure increase can be explained as follows. Just before the helium injection, there was some excess of condensation capability due to the decreasing decay power level. A small amount of air had accumulated in the lower part of the condenser, and had blanketed part of the active condenser surface. However, there was obviously not sufficient air available for blanketing and, consequently, the DW pressure began to decrease. Eventually, this process would have ended up with VB opening. But, at this time, the helium injection started. Helium injection and insufficient PCC performance re-

sulted in DW pressure increase, and subsequent venting, which provided good conditions for condensation in the PCCs.

In Test P5, air injection (28 g/s) was also started four hours after test initiation but, in this case, lasted only 0.5 hours. Because of the different facility configuration, the air mixed immediately with the steam injected in DW1, and was conveyed mainly to PCC1. From there, the air was vented to the SC. As a consequence, a significant system pressure increase in Test P5 occurred right after air injection began (see Fig. 3).

Practically all air was vented to the SC in Test P5, and the maximum possible system pressure increase was achieved. In Test P7, however, part of the helium remained in the upper part of DW1 until the end of the test, and did not contribute to the system pressure increase. With regard to containment integrity, the increase in system pressure is the more significant issue, while PCC performance is only indirectly affected by system pressure. With increasing system pressure, the steam is released from the RPV at higher (saturation) temperature, and the temperature difference between the PCC gas and the water on the PCC pool side increases. This larger temperature difference helps to improve the condenser efficiency during the non-condensible injection phase. Later, with decreasing decay power, the condenser efficiency should be sufficient, in any case.

### 3.3 Non-Prototypical Energy Transfer from the DW to the SP

As indicated above, the SC pressure had always been slightly increasing from the beginning of the tests. An explanation of this phenomenon can be given as follows. Because the heat removal capability was deliberately exceeded at the beginning of both Tests P5 and P7 (only two PCC units were connected, instead of three), venting through the main vent lines occurred. During main venting, steam was dumped directly to the SP, and practically all non-condensibles were purged from the main vent lines. Later in the test, main venting, and later still also PCC venting, stopped as a result of decreasing decay heat power. However, the main vent lines were filled with pure steam down to the bottom, and part of this steam was condensing inside the lines in the submerged region. Due to this condensation, the SP water surrounding the main vent lines was being heated, and eventually rose to the SP surface. The condensate itself, after leaving the vent lines from the bottom, was also rising, and accumulating at the SP surface, since its temperature was still higher than that of the surrounding water in the SP.

Direct heating of the SC gas space from the vent lines passing through the SC gas space was negligible for the following reasons. While, on the one hand, the vent line wall temperatures followed exactly the vent line gas temperatures, which indicated steam saturation conditions at the DW pressure, the SC gas space was not being heated significantly. On the other hand, the SP water temperature was increasing, showing at the same time stable temperature stratification. Furthermore, the lowermost SC gas temperature indication followed the SP surface temperature within a few degrees K. Based on these observations, we can assume that the SC gas space was heated by steam evaporation from the SP surface.

The described phenomenon can be considered as an additional energy transfer mechanism from the DW to the SP. However, this mechanism is not prototypical, because it would be impossible to valve off some of the PCC units in the ESBWR containment, and therefore main venting would not occur during the long-term cooling phase. In addition, the design of the PANDA vent lines is somewhat simplified: they consist of straight steel pipes passing through the SC gas space and submerged in the SP. Consequently, heat transfer was certainly increased, mainly in the submerged region.

## 4 PCC PERFORMANCE

### 4.1 Evaluation of PCC Performance

In the course of Tests P5 and P7, PCC performance varied considerably. In the first, essentially "undisturbed" test phase (i.e., before additional non-condensible gases were injected), the total PCC performance followed the decreasing decay power curve. As soon as large amounts of non-condensibles were conveyed into the condensers, the PCC performance was significantly degraded. After the non-condensible injection was stopped, the PCC efficiency improved again.

In the following, we will evaluate the transient PCC performance in PANDA in comparison to the main heat source, and other significant energy sinks observed in Tests P5 and P7. The energy input in the RPV is mainly used for raising steam. The steam is conveyed through the blow-down lines to the DW vessels, from where it enters the PCC feed lines, possibly mixed with non-condensibles. The steam condenses in the PCCs, and the condensate returns directly to the RPV. The non-condensibles are vented to the SC, if necessary. We will restrict the evaluation of the energy balances to a sub-system comprising the main energy flow path: i.e., to the RPV and the DW vessels to which the PCCs are connected. The SC serves as an energy and mass sink with regard to the RPV/DW vessel arrangement selected for this investigation. Furthermore, we assume steam at saturation conditions, which is consistent with the observations in Tests P5 and P7.

Under steady-state system pressure conditions, we would expect the overall heat losses from the facility to be the only additional heat sinks beside the condensers themselves. The heat losses from the RPV (below 5 kW), and from both DW vessels (below 15 kW), are small compared to the total reactor power. However, a non-prototypical energy transfer from the DW to the SP through the main vent lines was observed, as described in Section 3.3. This energy sink was revealed by a slowly decreasing water inventory

in the RPV. The condensate of the steam condensing in the main vent lines (and also in the DW vessels due to heat losses) was not returned to the RPV.

System pressurization was essentially caused by non-condensible venting to the SC gas space during or right after the non-condensible injection. In test periods with system pressurization, part of the energy was consumed for heating the RPV water, to follow the saturation line. At the same time, the RPV vessel and internal structures were being heated. Consequently, less steam was produced in the RPV. In addition, a certain amount of energy was needed for DW wall heating during the pressurization phase. Therefore, some portion of the steam/water was taken out of the "recirculation loop" between RPV and PCCs and was trapped in the DW vessels. This effect provides another contribution to the RPV level decrease: i.e., the RPV water inventory was reduced due to non-prototypical steam condensation in the main vent lines, and due to DW wall heating during pressurization transients.

To derive the energy balances, based on test data, simplifications were made with regard to the energy balance equation, and some terms, which appeared to be less significant for the tests being analyzed, were neglected. For example, the term representing the changes in total pressure was small in comparison with the other terms, and was therefore not considered. The changes in the RPV steam and DW gas enthalpy, in particular, during the non-condensible injection phase (pressurization), were also not considered. The changes in RPV water density during the moderate pressurization phase were similarly neglected.

On the other hand, the energy balances are based on spline fits of measured data, and their gradients. Locally measured values were used for calculating the thermodynamic fluid properties in certain facility regions. Although all steps in the procedure were carried out very carefully, we must be aware that we can only obtain an approximation to the items contributing to the energy balance. However, the sum of all independently determined sources and sinks should give a good indication of whether the results are acceptable or not.

The transient PCC performance was evaluated based on the decreasing pool water inventory. Energy balances derived from changes in pool collapsed level appeared to be more accurate than those obtained from feed or condensate flow measurements. During the long-term cooling phase, the PCC pool water was boiling at atmospheric pressure. The pool water was evaporating while it rose between the tubes of the condenser bundle, and flashing occurred above the condenser. At the pool surface, saturated steam was leaving the pool, and water was continuously recirculating. The water temperature corresponded essentially to the saturation temperature at atmospheric conditions.

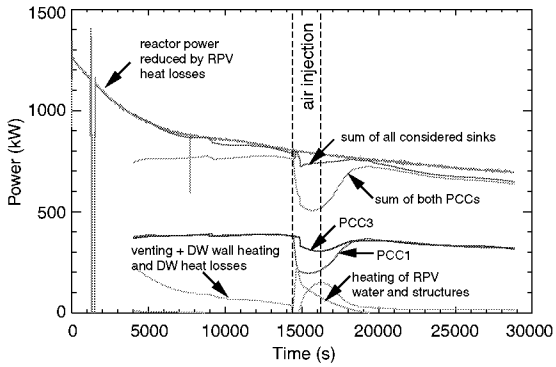


**Fig. 5:** Test P5 – energy source and sinks

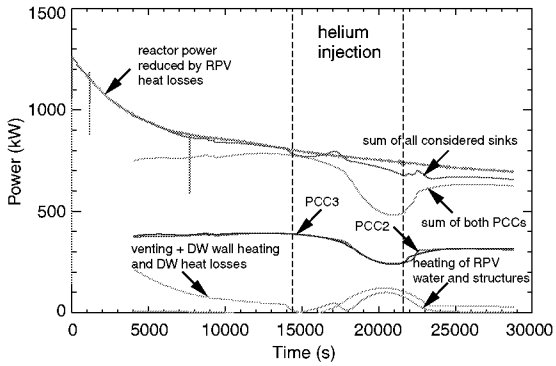


**Fig. 6:** Test P7 – energy source and sinks

Only a very small amount of water could be heated to temperatures above the atmospheric saturation temperature while it was rising between the tubes, and this amount was most likely constant. The heat losses from the PCC pools were negligible, as was demonstrated already in other tests. Calculating the pool water inventory, the structures in the pool, e.g. the condenser, were also considered. The total amount of energy transferred from the DW to the SP by steam condensation in both main vent lines, and the energy needed for DW vessel wall heating, but also for compensating the DW heat losses, was estimated based on the decreasing RPV water inventory. The RPV fluid and wall temperatures served as a basis for calculating the energy needed to follow the water saturation line, and to heat the RPV vessel and structures during system pressurization. The early test phase is not included in the following discussion, though the calculated energy balances are reasonable for this test phase too.

During the long-term cooling phase, i.e. before non-condensible injection was started, the PCC performance is practically identical in both tests, and is close to 400 kW for each condenser (see Figs. 5 and 6). The system pressure did not change in this test phase, except for a very modest increase due to the DW to SP energy transfer. Therefore, it can be assumed that the losses in RPV water inventory were primary caused by the energy sink in the main vent lines. Main vent clearing occurred at the beginning of

the test because of the insufficient heat removal capability of the two operating PCCs instead of three. Consequently, the changes in the slope of the decreasing RPV level were consistent with the changes in the main vent clearing frequency.

In Test P5, at the beginning of the air injection phase, the performance of PCC1, connected to DW1, where the non-condensibles were added, dropped almost immediately to about 50% (see Fig. 5). During this time, the air was mixing with the steam discharged from the blow-down lines, and was being transported to the condensers. The performance of PCC3, connected to DW2, decreased less, and also later in time. Obviously, only a small amount of the injected air was passing through the DW connecting pipe from DW1 to DW2 and mixing with steam.

With the relatively steep system pressure increase after air injection, a significant fraction of the decay heat was necessary to heat the RPV water and structures. The RPV water inventory losses increased temporarily as long as the system pressure increased, indicating that the DW walls were being heated due to steam condensation, and a larger amount of steam was vented to the SP due to the reduced PCC performance. The air injection did not only cause another main vent line clearing, but also PCC venting, which additionally contributed to the RPV water level decrease.

After air injection stopped, all air was vented from the DWs to the SC within approximately 2000 seconds. Later, the condenser tubes were blanketed with air in their lower parts, indicating excess heat removal capacity. Moreover, the DW to SC pressure difference was slightly decreasing; i.e., there was not sufficient air available for blanketing the condenser tubes in accordance with the decreasing decay power. Significantly less energy was transferred through the main vent lines after air injection. The SC pressure was decreasing slightly because the SC heat losses were obviously exceeding the energy transferred from the DW to the SC. The main vent lines, in particular main vent line 1 (connected to DW1) received part of the injected air, as indicated by the temperature readings.

In Test P7, at the beginning of the helium injection phase, the helium was almost exclusively accumulating in the upper part of DW1, showing little effect on the performance of the two operating PCCs, which were connected to DW2. Just before helium injection, the condensers showed some excess condensation capability and, due to the lack of non-condensible gases for blanketing the condenser surface, the DW pressure and the DW to SC pressure difference decreased slightly. The helium injection caused the DW pressure to increase slowly, and part of the decay heat was used to heat the RPV water and structures, as well as the DW walls. At the same time, a small amount of helium was conveyed to the PCCs and, consequently, PCC performance declined (see Fig. 6).

After helium transfer through the DW connecting pipe was detected by gas temperature readings in the connecting pipe, the DW to SC pressure difference increased more rapidly until PCC venting became possible; further system pressure increase was determined by the amount of vented non-condensibles. The main vents cleared soon after PCC venting occurred. The helium was obviously well mixed with steam in DW2, and performance degradation was similar in both PCCs. The minimum performance of both condensers during helium injection was about 500 kW. A similar value was obtained for Test P5. However, the operating conditions of the individual PCCs were very different in the two tests. As long as the system pressure was increasing, part of the energy was consumed for RPV water/structure and DW wall heating, as well as for steam condensation in the main vent line. We have to consider that the PCCs vented a steam/helium mixture at higher temperatures than in the air tests. This is most probably the reason for the difference in the appropriate terms of the energy balances for both tests after non-condensible injection was stopped.

After helium injection was stopped, the PCC performance increased in accordance with system needs. The helium/steam mixture trapped in the upper region of DW1 was slowly heated by the walls, and part of the mixture was released to DW2, from where it was vented. Gas temperature stratification in the DW connecting pipe indicated gas exchange between both DW vessels, and PCC venting was observed until the end of Test P7. Eventually, the system pressure increased moderately.

In both Tests (P5 and P7), temperature stratification of the SP water was terminated by non-condensible venting. The venting of large amounts of non-condensibles supported progressive mixing of the pool water. Therefore, the effect of the non-prototypical energy transfer from the main vent lines to the SP on system pressure practically disappeared. After the non-condensible injection was stopped, pool temperature stratification was not reestablished. Obviously, even low vent flow rates containing non-condensibles were sufficient to keep the water mixed.

The agreement between the sum of all energy sinks considered with the decay heat curve is obviously better before non-condensible injection in both tests, whereas an error of about 8% can be observed at the very end of the tests. The error arises mainly from the method used to calculate gradients of measured values: the first derivatives of splines fitting the measured values for water levels and temperatures were taken to calculate the changes in mass/energy and heat capacity; i.e., the absolute value of each gradient determined the value of the appropriate heat sink. We expected increasing relative errors with decreasing gradients: e.g., with less rapidly dropping water levels, the accuracy of the energy balances is also decreasing. The applied method is well suited for evaluating the energy sinks and their changes during the transient for engineering judgements of the system behaviour.

The evaluation of the main energy sinks in PANDA Tests P5 and P7 showed that the major fraction of the energy is removed by the PCCs in all test phases. However, the injection of non-condensible gases caused a significant degradation of PCC performance. After non-condensible injection was stopped, both non-condensibles heavier (P5) and lighter (P7) than steam could be vented from the condensers, which resumed operation on a relatively high level. The slight pressure increase at the end of Test P7 was caused by non-condensible venting. While PCC performance was degraded, part of the steam was vented to the SC, together with the non-condensibles. However, this kind of steam venting did not significantly contribute to the system pressure increase because the SP water was well mixed by the vented non-condensibles, and therefore the maximum amount of steam was condensed.

### 4.2 PCC Operating Modes and Non-Condensible Gas Distribution in the PCCs.

The energy balances for Test P7 showed that the PCCs were not blocked with helium. However, their performance was significantly degraded during the helium injection phase. Hereafter, the PCCs operated at part-load, in accordance with the decreasing decay power curve: i.e., the presence of helium was reducing PCC performance. While the adjustment of the active condenser surface by air accumulation is well understood from former experiments, Test P7 provided first data for the analysis of the transient PANDA PCC operating mode in the presence of non-condensibles lighter than steam. In this Section, the data of Tests P5 and P7 will be analyzed with regard to condenser operating modes and non-condensible distribution in the condensers.

The PANDA facility was well instrumented to make the interpretation of the measurements with regard to the overall system behaviour possible. Although the PCC tube regions were equipped with 23 (PCC1 and PCC2) or 35 (PCC3) temperature sensors, the instrumentation could not cover all details of the phenomena occurring in the tube bundle, which consisted of twenty tubes. The gas temperatures were measured in the central tube along the axis. At the same elevations, wall temperature sensors were installed at mid-wall thickness. Wall temperature and water temperature measurements were performed for another three tubes. The available instrumentation in the walls of parallel tubes allows, however, to draw some qualitative conclusions on the different performance in the tubes in one condenser, and/or between the condensers.

With decreasing decay power, system pressure cannot decrease because it is essentially bounded by the SC pressure. Previous tests performed with air showed that the PCCs adjust their performance by accumulating the non-condensibles heavier than steam in the lower region of the condenser tubes. However, excess heat removal capability can lead to DW pressure decrease, and subsequent short vacuum breaker (VB) openings. During vacuum breaker opening, a small amount of gas is returned from the SC, where mainly non-condensible gases (air) have collected, to the DW. Finally, these non-condensibles are conveyed to the condensers. A rather small amount of air is sufficient for adjusting the active condenser surface by tube blanketing; the rest is vented to the SC.

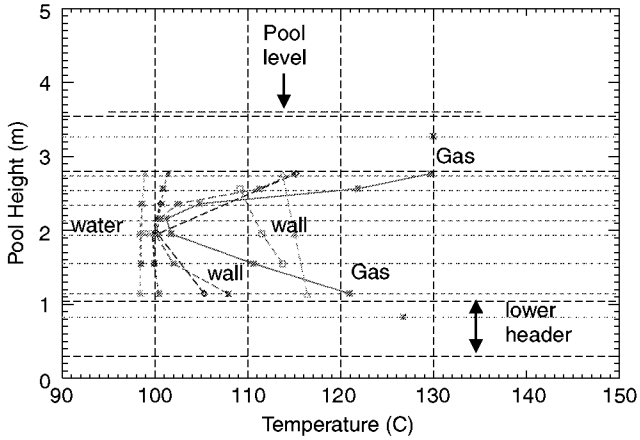


**Fig 7a:** Test P5 – axial temperature profiles in PCC3 at 20,000 seconds.

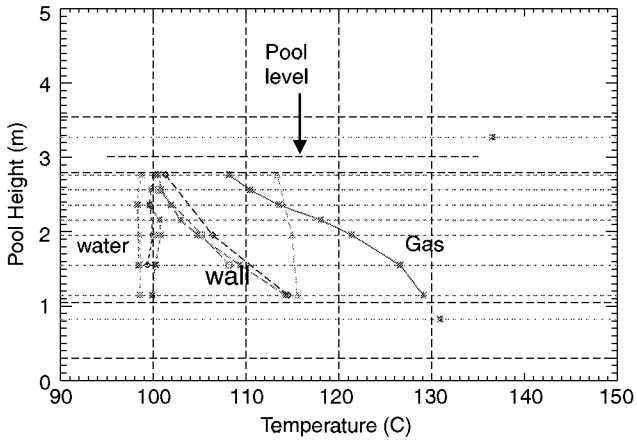


**Fig 7b:** Test P7 – axial temperature profiles in PCC3 at 16,700 seconds.

**Legend for Fig. 7a, 7b, 7c:**

Horizontal lines:

- black dashed lines: PCC upper and lower headers
- red dotted lines: thermocouple elevations
- green dotted lines: header gas thermocouple elevation
- blue dashed line: PCC pool water level

Gas, wall and water temperature measurements belonging to one tube have the same color but different line styles.

Gas, wall and pool temperature line styles:

- straight line: central tube gas temperature
- dashed lines: wall temperatures
- dotted lines: water temperatures

**Fig. 7c:** Test P7 – axial temperature profiles in PCC3 at 28,000 seconds.

Before the air injection phase in Test P5, excess heat removal capability was observed, and the DW to SC pressure difference slowly decreased. Consequently, the lower tube region of PCC1 filled with air at the beginning of the air injection phase. PCC3 was less affected, because it was connected to DW2, with no direct air injection. The air injection caused DW pressure to increase and, as soon as PCC venting became possible, almost all non-condensibles were vented from PCC1. Later during the course of air injection, the presence of air could be registered by the temperature readings at the tube outlets only (see Fig. 7a). The axial wall temperature profiles were similar in parallel tubes. Therefore, we assume that the axial gas temperature and air concentration profiles were also similar to the one observed in the central tube. Summarizing, the observations indicated gas stratification in the condenser tube bundle during the air tests, caused by the condensation process. The gas stratification led gradually to air blanketing of the condenser surface, beginning at the bottom of the bundle. Since the gas stratification causing the blanketing occurred in the relatively small volume of the condenser tubes, a small vent flow rate, or the addition of a small amount of air, was sufficient to adjust the active condenser surface. A gas mixture at the lowest possible temperature was vented from the lower header.

In the presence of helium (Test P7), a somewhat different behaviour was observed. Even before helium was first detected in the DW connecting pipe, the axial gas and wall temperature profiles in the central tubes of both PCC2 and PCC3 showed very low values at tube mid-height (see Fig. 7b). At this time there was sufficient condensation capability, and venting had not yet started. The wall temperature profiles in some of the parallel tubes were obviously not affected by this phenomenon: i.e., while some tubes were accumulating helium at mid-height, others were operating at higher rates, as shown in Fig 7b. Further, after venting started with increasing helium overflow to DW2, the axial gas temperature profiles in the central tubes showed a monotonic decrease from bottom to top. Comparing the axial wall temperature profiles of parallel tubes, we conclude that the tubes were still operating in different modes (see Fig. 7c). This behaviour did not change after helium injection was stopped because the temperature stratification in the DW connecting pipe indicated that the helium transfer from DW1 to DW2 had continued, but obviously at a lower level.

Summarizing the main observations, we can state that both the PCC feed and condensate flow rates and the energy balances proved that, during and after helium injection, the PCCs removed a significant amount of energy. At the same time, part of the gas mixture was vented from the lower headers to the SC. In addition, the difference of the gas temperatures in the upper and lower headers was very small compared to the test cases with air. Furthermore, we can distinguish two characteristic axial wall temperature profiles (see Fig. 7b and 7c). A typical wall temperature profile was practically uniform over the PCC height, at values close to the arithmetic average of the header gas and the pool water temperatures. Most probably, the steam/helium mixture was flowing down through these tubes. The second showed values decreasing from the bundle bottom to top. The central tube, which was instrumented on the gas side, belongs to the second group. The wall temperature readings at the lowermost elevation in the tubes practically coincide for both groups. Based on these observations, we conclude that the gas mixture flowing down in the first group of tubes enters the second group at the bottom. While the mixture in the second tube group was flowing from the lower to the upper header, a density and temperature gradient was established due to steam condensation, which was natural for a gas mixture consisting of steam and a non-condensible gas lighter than steam; i.e., the lower temperatures and higher helium concentrations were observed in the upper tube region. (In the air tests, lower temperatures and higher air concentrations were measured in the lower tube region, see Fig. 7a.) Part of the mixture enriched with helium was most probably leaving the second group of tubes at the top, the gas was then mixing with the feed flow in the upper header and flowing down again to the lower header through the tubes of the first group. Assuming steam saturation conditions inside the condenser tubes, the helium concentration was low in the first group of tubes where the helium was obviously well mixed with the steam.

The inclusion of tubes in one or other of the two characteristic groups is most probably dependent on small differences in their hydraulic characteristics. On the one hand, the tube lengths and shapes were slightly different, since the tubes were connected to horizontal cylindrical headers. On the other hand, a plate was installed in the upper header to intercept the jet entering from the feed line. Possibly, the condenser tube entries were approached at different angles, and with different velocities. In this context, it is interesting to note that one tube out of the four instrumented in PCC3 moved from the first to the second group during the course of the transient.

In summary, Test P7 demonstrated that gases lighter than steam can be successfully vented from the DW to the SC through the PCCs. The temporary degradation of condenser performance due to the helium content in the feed flow did not significantly contribute to the system pressure increase. Although, compared to air venting, helium venting was characterized by higher steam flows, at higher temperatures, a large portion of the vented steam was condensed in the SP. At the same time, the SP water was well mixed by the vented non-condensibles. In contrast to Test P5, in Test P7 the non-condensible helium was fed to the PCCs right to the end of the test. Consequently, conditions were not established at which the condenser could operate with pure steam flow at the entry, and without venting, but contained helium in the tubes and headers. However, with regard to the energy balances, the facility was close to this state at the end of Test P7. While in the tests with air the adjustment of

the active condenser surface was established by gas temperature stratification, similar in all parallel tubes, some kind of helium recirculation and load sharing between the parallel tubes was observed in the helium Test P7.

## 5 CONCLUSIONS

The response of the ESBWR PCCs to the addition of large amounts of non-condensibles lighter than steam (helium) during the long-term cooling phase was experimentally investigated in the large-scale facility PANDA. The measurements obtained from the Helium Test P7 were analyzed and compared with the Air Test P5 with regard to the influence of gas mixing on system pressure, to the degradation of PCC performance, and to the PCC operating modes.

It was found that the non-condensibles can accumulate in suitable DW regions due to gas stratification. In this way, the consequences of addition of non-condensible on system pressure could be mitigated. Further, it was demonstrated that helium can be successfully vented from the DW to the SC through the PCCs. The temporary degradation of PCC performance during the injection of non-condensibles did not significantly contribute to system pressure increase because the vented steam was, to the extent possible, condensed in the SP. In addition, the venting of non-condensibles destroyed the temperature stratification in the SP.

In the presence of helium, the PCCs were operating in a different mode compared with the air tests: some kind of helium recirculation and load sharing between the parallel tubes was observed in the helium test. Tests performed at different conditions are desirable to confirm the findings of this first ESBWR PCC test with non-condensibles lighter than steam, and more detailed instrumentation is desirable to improve understanding of the PCC operating mode in the presence of non-condensibles lighter than steam. However, the data obtained in the first helium system test is already suitable for containment code assessment.

## NOMENCLATURE

| | |
|---|---|
| DW | Drywell |
| ESBWR | European Simplified Boiling Water Reactor |
| PCC | Passive Containment Condenser |
| SC | Suppression Chamber |
| SP | Suppression Pool |

## ACKNOWLEDGMENTS

The work presented in this paper was supported by the European Commission in the Euratom Fourth Framework Program on Nuclear Fission Safety, and by the Swiss Federal Office for Education and Science. These financial contributions are gratefully acknowledged.

## REFERENCES

[1] Bandurski T., Dreier J., Huggenberger M., Aubert C., Fischer O., Healzer J., Lomperski S., Strassberger H.J., Varadi G., Yadigaroglu G., *"PANDA Passive Decay Heat Removal Transient Test Results",* Proc. of the 8th Int. Topical Meeting on Nuclear Reactor Thermal-Hydraulics, Vol. I, pp. 474-484, Kyoto, Japan, 1997.

[2] Huggenberger M., Aubert C., Bandurski T., Dreier J., Fischer O., Strassberger H.J., Yadigaroglu G., *"ESBWR Related Passive Decay Heat Removal Tests in PANDA",* ICONE-7322, Proc. of the 7th Int. Conf. on Nucl. Engineering, Tokyo, Japan, 1999.

[3] Schenk H.W., Hooft van Huysduynen A.M., *"Scaling Analysis of Passive Containment Cooling Tests",* INNO-TEPSS(96)-D004, ECN, Petten, 1997.

[4] Shiralkar B.S., Gamble R.E., Yadigaroglu G., *"Passive Containment Cooling System Performance in the Simplified Boiling Water Reactor",* Proc. of the Int. Meeting on Advanced Reactors Safety (ARS '97), pp 478-484, Orlande, Florida, USA, 1997.

[5] Shiralkar B.S., Healzer J.M., Petry A., *"Effect of Drywell Non-condensible Gas Distribution on Passive Containment Cooling System Performance",* ICONE-6522, Proc. of the 6th Int. Conf. on Nucl. Engineering, San Diego, USA, 1998.

[6] Yadigaroglu G., *"Derivation of General Scaling Criteria for BWR Containment Tests",* Proc. of the 4th Int. Conf. on Nucl. Engineering, New Orleans, USA, 1996.

[7] Yadigaroglu G., Dreier J., *"Passive Advanced Light Water Reactor Designs and the ALPHA Program at the Paul Scherrer Institut",* Kerntechnik, **63** 1-2, pp. 39-46, 1998.